LBL-35959
UC-410

Lawrence Berkeley Laboratory
UNIVERSITY OF CALIFORNIA

Accelerator & Fusion Research Division

Presented at the 1994 European Particle Accelerator Conference, London, England, June 27–July 1, 1994, and to be published in the Proceedings

Modeling of Beam Dynamics and Comparison with Measurements for the Advanced Light Source (ALS)

J. Bengtsson and M. Meddahi

June 1994

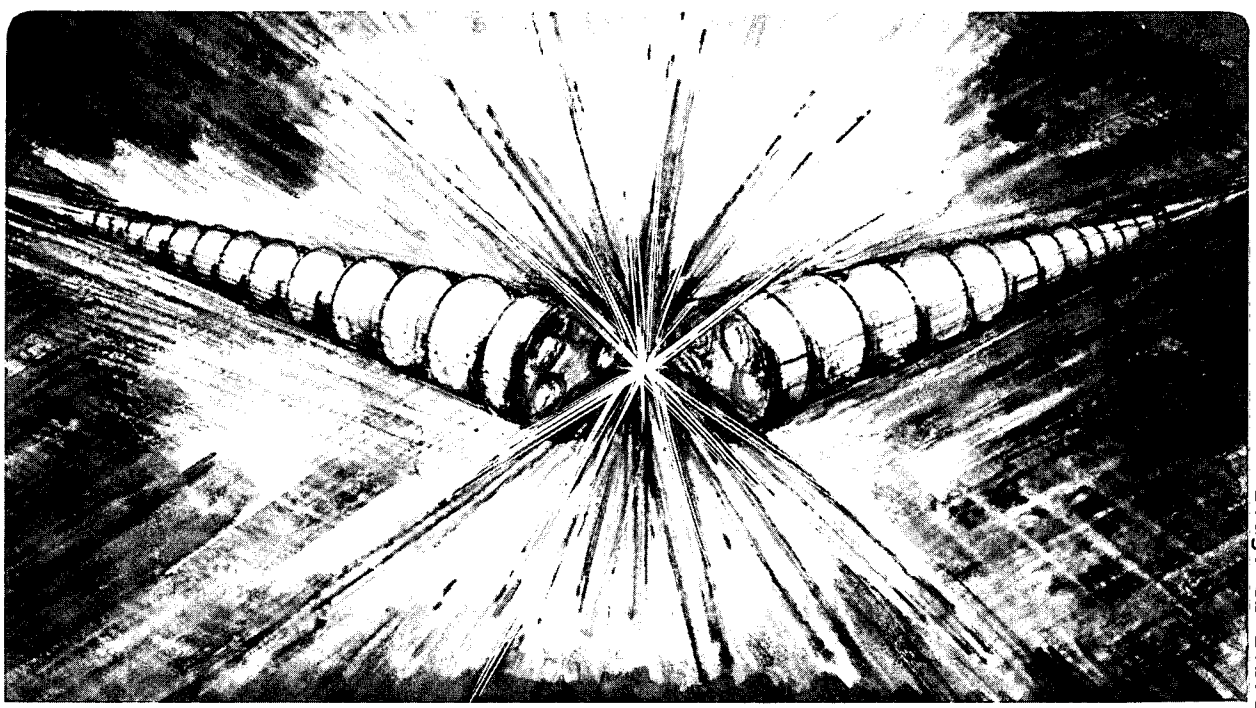

Prepared for the U.S. Department of Energy under Contract Number DE-AC03-76SF00098

DISCLAIMER

Modeling of Beam Dynamics and Comparison with Measurements for the Advanced Light Source (ALS) *

J. Bengtsson
LBL, M/S 71H, 1 Cyclotron Road, Berkeley, CA 94708
M. Meddahi
now at CERN-SL, CH-1211 Geneva 23

Abstract

The data collected during the April 1993 ALS commissioning period includes the measured closed orbit as a function of either dipole corrector strength or RF frequency, in addition to turn by turn data for the betatron motion as a function of RF frequency. The sensitivity matrix and dispersion function are extracted from this data by taking differences between orbits, whereas lattice functions and chromaticity are obtained using Fourier analysis and interpolation techniques. Lattice functions are also derived from the sensitivity matrix using a nonlinear least squares fit. The results are then compared with numerical simulations and analytical formulas derived using maps and a Lie product normal form approach. The Lie method is preferred to traditional Hamiltonian perturbation theory because it is easily generalized to the nonlinear case and also leads to a significantly reduced amount of algebra. The computer modeling uses state of the art single particle beam dynamics tools including: Tracy-2, DA-pascal, DA-library and Lie-Lib. In particular, DA-Pascal allows for a straightforward implementation of a Krakpot style code, based on the "exact" single particle local Hamiltonian and a symplectic integrator, necessary for correct modeling of the nonlinear chromaticity.

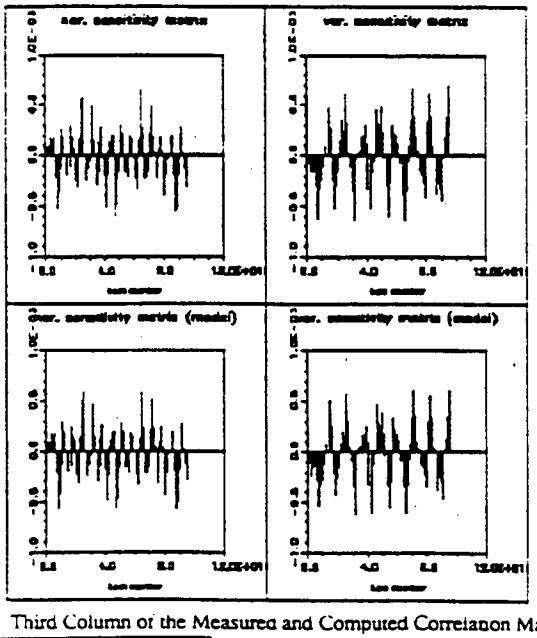

Fig.1 Third Column of the Measured and Computed Correlation Matrix

*This work was supported by the Director, Office of Energy Research, Office of High Energy and Nuclear Physics, High Energy Physics Division, of the U.S. Department of Energy under Contract No. DE-AC03-76SF00098.

1 Sensitivity Matrix

The linear sensitivity matrix S is defined by:

$$\Delta\bar{x}_{cod} = S\bar{\Theta} + O(1), \quad S = \frac{\partial\bar{x}_{cod}}{\partial\bar{\Theta}}|_{\bar{\Theta}=\bar{\Theta}_{ref}} \tag{1}$$

with S the Jacobian. The sensitivity matrix describes the change of the closed orbit at a certain location due to dipole kick at some other location. An analytical expression of the sensitivity matrix is given by [1]:

$$S_{ij} = \frac{\sqrt{\beta_{xi}\beta_{xj}}\cos\left(\pi\nu_x - |\mu_{xj} - \mu_{xi}|\right)}{2\sin\pi\nu_x} - \frac{\eta_{xi}\eta_{xj}}{\alpha_c C} \tag{2}$$

where β is the beta function, μ the phase advance, η the dispersion function, ν the tune, α_c the momentum compaction, C the circumference and x the transverse coordinate. Comparison between one column of the measured and computed matrix shows excellent agreement as seen in Fig. 1 and allows for diagnosis of mal-functioning hardware (BPMs and correctors) [2].

2 Extraction of Linear Lattice Functions

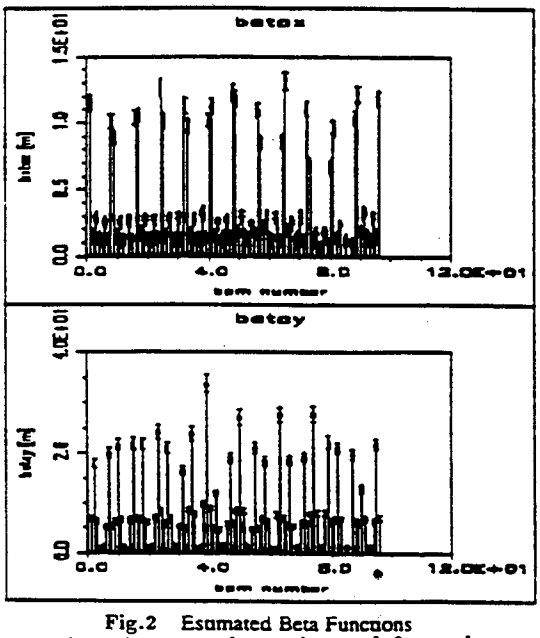

Fig.2 Esumated Beta Functions

The lattice functions can be estimated from the measured sensitivity matrix by a nonlinear least square fit in both the horizontal and vertical plane [1]. The system of nonlinear equations is solved iteratively using the Levenberg-Marquardt method. Due to the lack of space, only the beta function is plotted in Fig. 2. The error bars indicate a 95.4 % confidence interval. The estimated tunes

are $\nu_x = 14.341 \pm 0.0005$ and $\nu_y = 8.316 \pm 0.0005$ and the final standard deviation are: $\sigma_x = 2.2 \times 10^{-5}$ and $\sigma_z = 1.7 \times 10^{-5}$. Simulations with Tracy-2 shows that expected gradient errors are not sufficient to account for the observed magnitude of the perturbations of the beta function. However, closed orbit distortions in the sextupoles will also contribute due to feed down. A nonlinear least square fit of this contribution leads to reasonable values when compared to the BPM readings. The corresponding beta function is shown in Fig. 3.

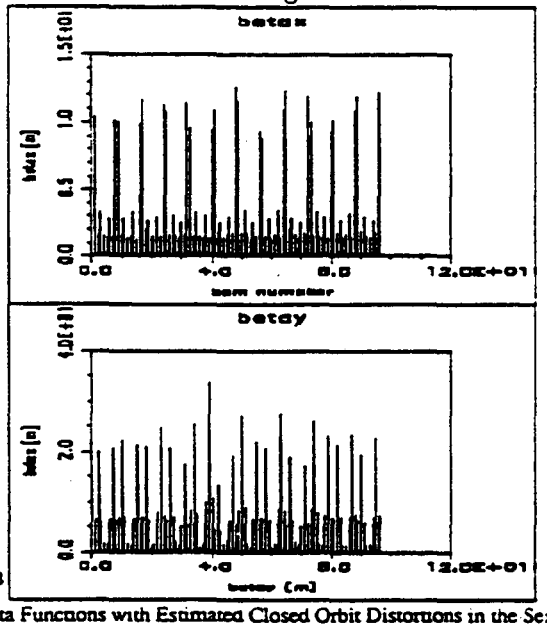

Fig.3 Beta Functions with Estimated Closed Orbit Distortions in the Sextupoles

3 Analysis of Linear Dispersion Function

Analytical Model

If one adds a normal and skew quadrupole kick to the initial one-turn map [1], one finds (with $\vec{\xi}$ the transfer map, $\mathcal{M}$ the corresponding functional map, $(x,\ y)$ the transverse coordinates, L the magnet length and b_2 the multipole coefficient):

$$\begin{aligned} \mathcal{M}_{\vec{\xi}_{i-N+1}} &= \mathcal{M}_{\vec{\xi}_{i-N}} e^{:-\frac{(b_2L)_1}{2}(x^2-y^2):} \\ &= \mathcal{L}_1^{-1}\mathcal{R}e^{:-L_1\frac{(b_2L)_1}{2}(x^2-y^2):}\mathcal{L}_1. \end{aligned} \quad (3)$$

The map in Lie product normal form is:

$$\mathcal{M}_{\vec{\xi}_{i-i+N+1}} = \mathcal{L}_i^{-1}\mathcal{R}_{j-i}^{-1}\mathcal{K}_j^{-1}\mathcal{R}e^{:h:}\mathcal{K}_j\mathcal{R}_{j-i}\mathcal{L}_i \quad (4)$$

where:

$$\begin{aligned} \mathcal{K}_j &= e^{:-\frac{1}{1-\mathcal{R}^{-1}}\frac{(b_2L)_j}{4}[\beta_{xj}(x^2-p_x^2)-\beta_{yj}(y^2-p_y^2)+4\eta_{xj}\sqrt{\beta_{xj}}\delta x]:}, \\ h &= -\frac{(b_2L)_i}{2}(\beta_{xj}J_x - \beta_{yj}J_y + \eta_{xj}^2\delta^2) \end{aligned} \quad (5)$$

It follows that the tune shift is given by:

$$\Delta\nu_{x,y} = -\frac{1}{2\pi}\frac{\partial h}{\partial J_{x,y}} = \pm\frac{(b_2L)_j\beta_{x,yj}}{4\pi} \quad (6)$$

as expected. This allows one (well known) to measure the beta function at a quadrupole by changing the gradient and observing the change in tune. The perturbation of the trajectory is given by:

$$\begin{aligned} \mathcal{K}_j\mathcal{R}_{j-i}\mathcal{L}_i\vec{x} &= e^{:-\frac{1}{1-\mathcal{R}^{-1}}(b_2L)_j\eta_{xj}\sqrt{\beta_{xj}}\delta x:} \\ &\quad \times\mathcal{R}_{j-i}\mathcal{L}_i\vec{x} + O(2), \quad j<i \end{aligned} \quad (7)$$

and the change of the closed orbit is:

$$\Delta x_i = (\kappa_j\mathcal{R}_{j-i}\mathcal{L}_i x)(0,\delta), \quad \Delta y_i = (\kappa_j\mathcal{R}_{j-i}\mathcal{L}_i y)(0,\delta) \quad (8)$$

so that the perturbation of the linear dispersion function is given by (similar expression in the y plane):

$$\Delta\eta_{xi} = -\sum_j \frac{(b_2L)_j\eta_{xj}\sqrt{\beta_{xi}\beta_{xj}}\cos(\pi\nu_x - |\mu_{xj}-\mu_{xi}|)}{2\sin\pi\nu_x} \quad (9)$$

It follows that a normal quadrupole component changes the horizontal dispersion whereas a skew quadrupole component changes the vertical. Note that the perturbation is beating with the tune in each plane around the lattice.

Data Analysis

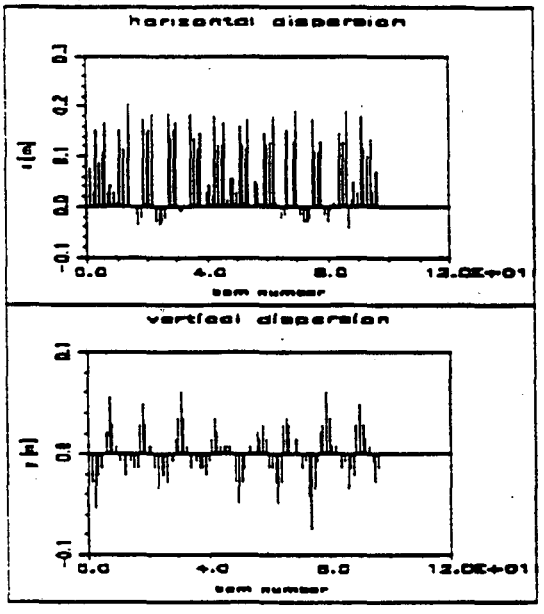

Fig.4 Measured Linear Dispersion Function

The RF frequency was swept from 499.65408 MHz to 499.66600 MHz in increments of 1 kHz and the closed orbit recorded for each frequency. The linear dispersion is extracted from the data by numerical differentiation. The measured dispersion is shown in Fig. 4. Note the beating of the perturbation with the tune in each plane as predicted from the analytical model and the contribution from normal as well as skew (vertical) quadrupole components. Numerical simulations reveals that realistic quadrupole tilt and gradient errors can not reproduce the data. Furthermore, major gradient errors could not by themselves reproduce the data, since they do not contribute to the vertical dispersion. However, the dispersion obtained by a nonlinear least square fit of the closed orbit in the sextupoles to the measured dispersion is shown Fig. 5. It follows again that reasonable closed orbit distortions

in the sextupoles accounts for the measured perturbations of the linear dispersion function.

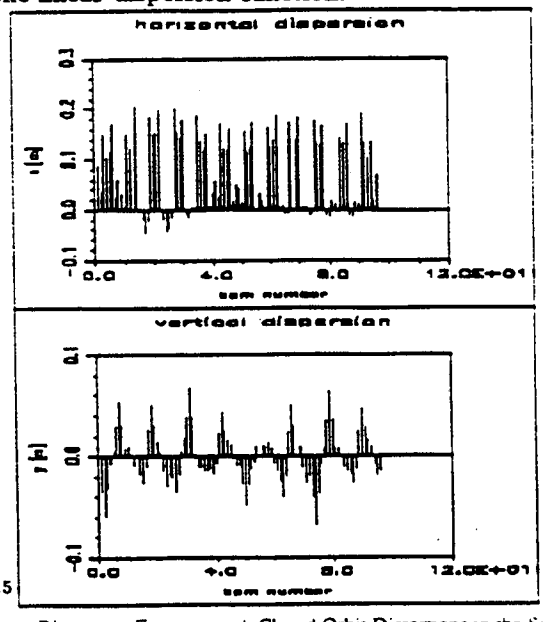

Fig.5 Linear Dispersion Function with Closed Orbit Distortions in the Sextupoles

4 Nonlinear Chromaticity

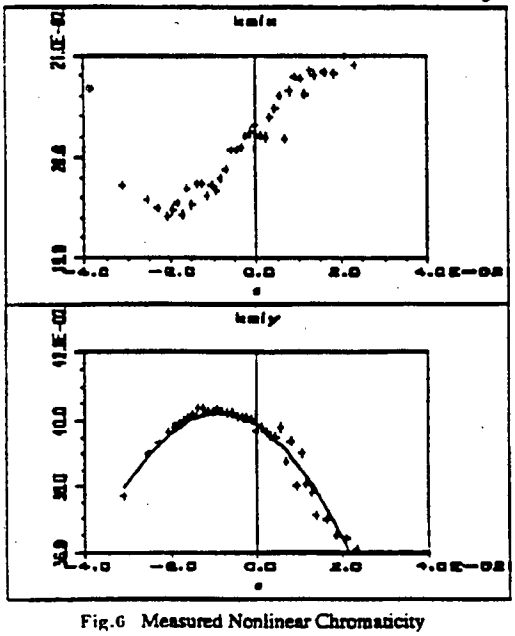

Fig.6 Measured Nonlinear Chromaticity

The measured initial tunes were $\nu_x = 14.201$ and $\nu_y = 8.415$. The RF frequency was swept from 499.63556 MHz to 499.69110 MHz in approximately 1 kHz increments. The linear and second order chromaticity are extracted by a linear least square fit of a polynomial to the data. The results are shown in Fig. 6 where plus signs represent the data and the solid line the result of the fit. Defining:

$$\nu_x \equiv \nu_{x0} + \xi_{x0}\delta + \xi_{x1}\delta^2 + O(\delta^3) \qquad (10)$$

one finds: $\nu_{x0} = 14.20116$, $\nu_{y0} = 8.39754$, $\xi_{y0} = -0.77920$, $\xi_{y1} = -43.903$ with a sigma of $\sigma_y = 3.1 \times 10^{-3}$. The extremum has been shifted in the horizontal plane due to a finite linear chromaticity preventing a good fit.

Tracy-2 is using the expanded Hamiltonian, a thin quadrupole for the bend edge focusing and neglects quadrupole fringe fields. This model does not give the correct chromaticity (in the case of a small ring) and we investigated the quality of the model for a medium size ring like the ALS.

component (no sextupole)	order	x	y
Tracy-2	1	-24.89	-26.84
	2	33.97	66.68
improved Tracy	1	-24.89	-27.88
$(1/(1+\delta))$	2	33.97	70.64
Krakpot	1	-24.59	-27.68
prot	2	32.66	74.18
Krakpot (prot, n.l.	1	-24.78	-27.66
drift, quad.fringe)	2	34.91	75.67

Without sextupoles, "improved Tracy-2" refers to correction of the momentum dependence of the bend edge focusing. The second case was computed by implementing a Krakpot style code [3] by an input file with a symplectic integrator for DA-Pascal. The third case was obtained by using Dragt's "prot" [4] and hard edge approximation of the fringe field. For the fourth case, a nonexpanded Hamiltonian is used as well as hard edge quadrupole fringe fields. Tracy-2 gives a good estimate of the natural chromaticity. The value in the vertical plane is significantly improved with the corrected momentum dependence. We find that expanding the Hamiltonian and neglecting the quadrupole fringe fields are valid approximations for both the linear and second order chromaticities.

component (with sextupoles)	order	x	y
no higher order	1	1.00	-0.78
multipoles	2	-43.65	-67.86
all syst.higher	1	1.00	-0.78
order multipoles	2	-40.41	-57.28
only syst. octupole	1	1.00	-0.78
in Bend.	2	-45.03	-57.10

With chromatic sextupoles, there is a significant contribution to the second order terms, strong enough to even change the sign (only two families). In particular, the systematic octupole component in the bend, gives an additional contribution to the second order chromaticity in the vertical plane. The agreement with the measured value, when this contribution is included, is reasonable.

References

[1] J. Bengtsson and M. Meddahi, to be publ.

[2] J. Bengtsson and M. Meddahi, CBP Tech Note 003, 3/1/93.

[3] E. Forest et al., to appear in Part. Accel., vol. 45, issue (2-3), p. 65

[4] A. J. Dragt, Part. Accel. vol. 12, p. 205-218 (1982).

LAWRENCE BERKELEY LABORATORY
UNIVERSITY OF CALIFORNIA
TECHNICAL INFORMATION DEPARTMENT
BERKELEY, CALIFORNIA 94720